Chapter 2

Transition Metal Dichalcogenide Photodetectors

Inturu Omkaram, Young Ki Hong and Sunkook Kim

Additional information is available at the end of the chapter

http://dx.doi.org/10.5772/intechopen.72295

Abstract

Two Dimensional (2D) materials has triggered to have transition metal dichalcogenides (TMDCs) emerging as a new class of materials that can control or interact with light to convert the photons to electrical signals for its attractive applications in photonics, electronics and optoelectronics. 2D materials along with gapless Graphene interact with light over the wavelength region of the different spectral regions having the short wavelength of the UV and extreme UV, Visible, near IR, mid IR and THz due to excellent light absorption, enabling ultrafast and ultrasensitive detection of light in photodetectors. Next generation photodetectors are possible promising candidates for high sensitivity and TMDCs based photodetectors are the heart of the multitude of technologies to understand the principle of photodetection mechanisms and device performances. Phototransistors/photoconductors show wide varied detection performances with responsivities ranging from 10^{-7} A/W - 10^{7} A/W on single or few layer TMDCs having response time between 10^{-5} s to 10^{3} s. The semiconducting TMDCs like MoS_2, $MoSe_2$, WS_2, WSe_2 and ReS_2 are gaining suitable applications in optoelectronic devices and the device design, mechanism and enhancing the performance of photodetectors are introduced and discussed systematically in this chapter. In spite of the growing demands on TMDC based devices the origin of the photoresponse characteristics is attractive and encouraging to understand and provide a path to the subject of investigation and guidelines for the future development of this rapidly growing field.

Keywords: 2D semi-conductors, transition metal dichalcogenides (TMDCs), photodetectors, optoelectronic 2D devices

1. Introduction

Recently, 2D nanomaterials are rapidly expanding as one of the prime goal of materials research from different disciplines such as physics, materials science, chemistry and electrical

engineering. 2D materials with new entrants have been widely researched for its unique electronic & optoelectronic components, sensors, biomedical and drug delivery applications [1–5]. It is a fascinating counterpart to gapless graphene that has successful isolation, the ideas and methods have rapidly established from these early studies were prolonged to various layered materials [6–8]. Alike to graphite, the two dimensional crystals established on atomically thin films of layered semiconductors, such as the family of transition metal dichalcogenides (TMDCs) offer an attractive platform for various optoelectronic applications [9–21]. TMDCs are highly attractive due to the existence of an appropriate energy band gap (1.2–1.8 eV) that has numerous unique properties that can be synthesized into thick atomic planes when compared to the bulk counterparts. The semiconducting 2D metal chalcogenides are of peculiar interest with the essential possibilities to explore the band gap discoveries by varying the number of layers making them an exciting application for devices [7]. Investigations on band structure have dramatically changed from bulk layer to single layer samples having the direct band gap semiconducting TMDCs suitable for optoelectronic applications. The quantum size effects play a prominent role due to their nanosize in expressing the distinctive properties of the material that are not noticed in its bulk form having inspiring fascinating applications in the development of transparent and flexible optoelectronic devices [22–24].

In optoelectronics, graphene has been utilized for the realization of photodetectors and optical modulators. 2D materials offer complementary to graphene that lacks the interlayer interactions having potential applications in the nano and optoelectronics to evaluate their electronic band structure and their spaced energy levels [25–27]. Interest in two-dimensional (2D) TMDCs materials can be defined as any material in which the bond strength between atoms within a plane are much stronger than the bonds out of the plane that are exfoliated easily to present interesting electrical-optical behavior. Optoelectronics integrate the physics of light and these electronic devices can control light that converts photons or plasmons to electrical signals. When light is incident on a semiconductor, they create free carriers (electron-hole pairs) on the exciton binding energy in the semiconductor. The photon energy greater than the band gap is gained by the electrons that move the common barrier in between the metal and semiconductor, the energy gained by the electron which is called the work function is given by kinetic energy [28]

$$E_e = \frac{hc}{\lambda} - \phi_m \tag{1}$$

where λ is the incident wavelength, φ_m is termed to be the metal work function and C the light velocity. Since the photoelectric effect is based on the photon energy hν, the wavelength of interest is related to the energy transition ΔE in the device operation with this relationship $\lambda = \frac{hc}{\Delta E} = \frac{1.24}{\Delta E}$ (eV) μm where ΔE is the difference of energy levels transition. The discrete energies ΔE of the semiconductor causes the excitation with the greater photon energy and the bound excitons generate a photocurrent when it is separated by an applied electric field with two major classes of semiconductor photo detectors. The two categories are likely to be the photodiodes and phototransistors that are transparent and flexible thin film electronic

devices having its great importance in the transparent displays, UV Detectors, wearable electronics and solar cells [29–31].

There have been partial 2D discussion on the focus of TMDCs in recent years. This chapter examines the properties of 2D materials from a new perspective related to the optoelectronic properties of 2D materials. In a pioneering work of MoS_2 phototransistors the exfoliated single-layer exhibits a photoresponsivity of 7.5 mA/W at 50 V of the gate voltage [32]. Phototransistors founded on CVD MoS_2 multilayer by local bottom gate structures show a supreme responsivity of 342.6 A/W [33] and monolayer/WS_2 multilayers devices show a photoresponsivity value of 880 A/W and a photodetector with high detectivity of 2.2×10^{12}–7.7×10^{11} Jones and a maximum photoresponsivity up to 2570 A/W have been reported [17, 23]. The synthesis route and the structural characterization of TMDCs having fascinating properties of 2D materials provides a discussion of the TMDC-based devices with photoresponsivity, the main emphasis is on describing relevant methods and important outcomes as well as some of the novel applications of 2D photo detectors [34–36]. It is an intent to give a comprehensive overview of the recent experimental results related to 2D photo detectors and its applications. In particular, this chapter covers 2D photo detector materials synthesis and characterization, device (phototransistor) fabrication, mechanism, performance of phototransistors in optoelectronics. This method attempts to highlight the various synthesis approaches for 2D materials like bottom up synthesis routes including chemical vapor deposition (CVD), hydrothermal and layer-by layer conversation and bottom down approaches like chemical or mechanical exfoliation had their corresponding characterization by which the current understanding of 2D materials has some tools for future contributions. The achievement of 2D materials created explosive interest to enrich the performance of TMDC photo detectors, having the practice of periodic elements challenges novel discoveries for the exciting new physics and ultimately thin devices.

2. Synthesis methods for 2D materials

2D TMDCs can be divided into two groups as

(2.1) top down

(2.2) bottom up.

With top down approaches, there are mechanical and chemical exfoliations. In mechanical exfoliation the approach starts from bulk TMDC materials which naturally comprise of many layers where scotch tape is used to peel nanosheets of bulk TMDCs. It has advantage of producing high purity and clean single crystal flakes but still limited to control the size and thickness as the materials are easy to crack owing to grain margins, material flaws and process prompted stress. For chemical exfoliation, ion assisted exfoliation can be used. Bulk TMDCs powder is submerged in lithium ion containing solution (like n-butyllithium) and the lithium ion to intercalate into the bulk TMDCs. The intercalated material is exposed to water and water will react vigorously to evolve H_2 gas with in the lithium layers thus separating the layers

rapidly producing high yield of monolayer TMDCs. It also failed to enlarge the size of the monolayer which will restrict in practical applications.

The label bottom up approaches itself notates to construct from the bottom and the best methods are physical vapor deposition (PVD)/Chemical vapor deposition (CVD). In PVD, the bulk TMDCs is frenzied in a tube furnace until it thermally evaporates. A flow of inert gas would carry the vapor stream to a cooler region and deposit it on to the substrate. Single crystals are developed with grain dimension of several tens of micrometer, additionally layer number can be controlled by varying the amount of precursor used. In CVD two precursors are used (1) transition metal compound (M) (2) chalcogenide (X) precursor, the chalcogenide is placed upstream in the tube furnace at a lower temperature than the transition metal compound at higher temperature region in the tube furnace downstream. The furnace heats up so that the precursors are thermally evaporated, reacts to form MX_2 and is deposited on a substrate which is further downstream as compared to transition metal compound with inert gas as carrier gas. The advantage of CVD growth is that large area uniform polycrystalline thin film (cms) are grown with a possibly to grow single crystal by varying precursors.

2.1. Top down approaches

2.1.1. Mechanical exfoliation

It is a topdown method that is proved to be quite successful that is most traditional and simplest to prepare high quality single layer of graphene and TMDCs materials. Geim and Novoselov [37] used a block of graphite by cleaving it into different layers of graphene and transferring it onto the substrates using scotch tape. The TMDCs samples are prepared by peeling off from their parent bulk crystals with micromechanical cleavage by adhesive tape as shown in **Figure 1(a)**. This process was quick, cost efficient and the tape was repeated—peeled material is applied to a substrate. Geim and Novoselov [37] cleaved the layered and revealed that this method can also be applied to Boron Nitride &TMDCs [12].

Due to some limitations in this method of mechanical cleaving, the morphology control was not systematically carried with flake size, the thicknesses of the nanosheets obtained were small and tens of microns, it's a problematic for massive production outside the laboratories has its own limitations in applications.

2.1.2. Electric chemical exfoliation

It is an effective topdown method that is inspired by the exfoliation methods that was advanced where lesser Li ions being charged are intercalated to different layered TMDCs bulk materials. Zheng et al. [38] developed the bulk TMDCs is positioned on the cathode and a lithium intercalated material were in the electrolyte (water or ethanol) as shown in **Figure 1(b)**. In this set up charge is allowed to pass and the enforcement of the charged ions in the layered material by intercalating the cathode. Lithium ions are induced inside the layers of TMDC materials at change and Hydrogen gas is produced when the intercalated bulk material is reacted with water in sonication to obtain the 2D TMDCs [13]. This separates the TMDC layers during charging process and require low temperature to fully control the procedure by

http://dx.doi.org/10.5772/intechopen.72295

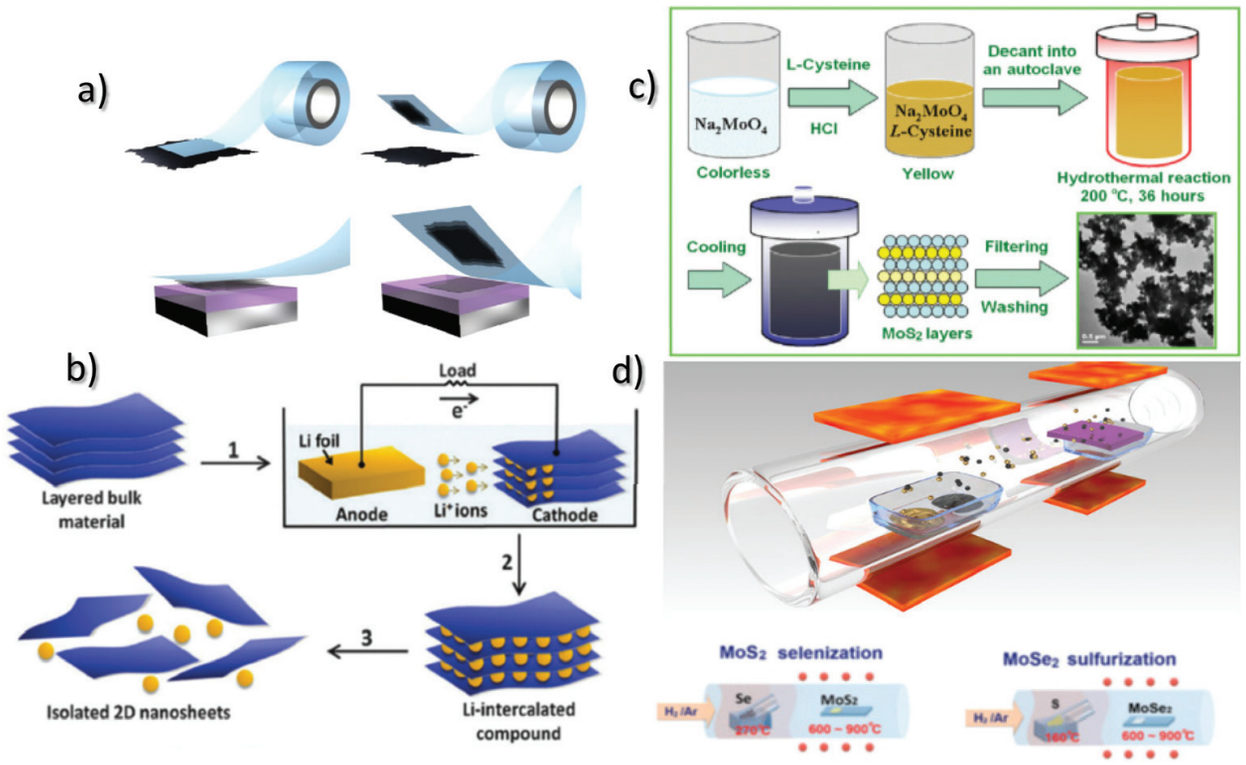

Figure 1. (a) Mechanical exfoliation method. (b) Lithiation and exfoliation process in a lithium ion battery system. (c) Preparation of MoS_2 with the use of a simple hydrothermal method. (d) Synthesis of the hexagonal $MoSe_2$ multilayer nanoparticles with MoO_3 and Se sources and the experimental set-up of the selenization and sulfurization process. Adapted from Novoselov and Castro Neto [12], Zhang et al. [13], Guo et al. [39], Jung et al. [99], Shi et al. [14].

referring to a discharging curve. The disadvantage by these intercalation methods is due to the impurities lead to the modifications in the electrical properties.

2.2. Bottom up approaches

2.2.1. Hydro-thermal method

It is an owing bottom-up technique for synthesis of two-dimensional TMDCs. It is normally supported in a pressurized autoclave with the reactions in aqueous solutions to procedure TMDC layered single crystal [39] as depicted in **Figure 1(c)**. The temperature and pressure on the solution in an autoclave can be elevated to the boiling point of water and touched to the pressure of a vapor saturation. MX_2 TMDC layered material, for instance, is produced by adding Mo, W and S, Se into autoclave and heating in the noble gas (For example N, Ar) to 773 K for 3 hours. The hydrothermal method can produce high quality of TMDC material with uniform size (from several nanometers to several microns) but the thickness of TMDC wafer cannot be controlled.

2.2.2. Chemical vapor deposition

Chemical vapor deposition: CVD is an employed technique currently used in the synthesis of graphene and 2D TMDC materials that are exploited in the study of nanostructures including

thin films and nanotubes. It is also another bottom-up method that realizes chemical reaction between vapors to form TMDC wafers at high temperature. It is one of the supreme well-organized ways to gain and grow large films on a substrate [40]. In order to form a two-dimensional material, normally, precursor is applied (S, Se and MoO_3, WO_3) on high temperature region and substrate (sapphire or SiO_2/Si substrate) on low temperature region in a pipe furnace. **Figure 1(d)** shows the procedure for 2D TMDCs [14] synthesis depends on evaporating of Sulfur;Se and MoO_3;WO_3.

The vaporized solid was then deposit on substrate to form a 2D TMDC crystal. It is the most operative way to form large area, high quality TMDCs and achievable method in thickness controlling. Other CVD methods entails the Mo sulfurization or a reagent rich in sulfur atmosphere on the substrate are used for the synthesis of 2D MoS_2 materials. The thickness and homogeneity of these 2D MoS_2 is regulated having more restrictions on the large area is not achieved and not controlled precisely. Therefore, it is preferred alternative for synthesis of 2D TMDCs material for electronic and optical device fabrication.

3. 2D transition metal dichalcogenides

Transition Metal Dichalcogenides; TMDCs; as 2D semiconductors are proposed to be a layered periodic part of elements consists of transition metal (Mo or W or Re) and chalcogen (S or Se or Te) atoms frequently represents as MX_2, where M is transition metal (usually group V/VI element) and X is Chalcogen [15, 41–44]. TMDCs provide novel and outstanding phenomena varying from indirect to direct band gap transition, large exciton binding energy, photoluminescence and high ON/OFF ratio which are particularly changed from those of their bulk materials.

The bulk material is significantly different from the nano-scaled particles that are divided into numerous categories based on dimensional topological spacing difference such as OD, 1D, 2D & 3D nano materials. 2D materials are crystalline materials containing of layered arranged atoms/molecules which has strong covalent bonds within each layer but only weak Vander Waals forces between layers that novelties application such as electrode, semiconductors and photovoltaics [9, 45].

In 2004, the production of thin carbon layer by mechanical exfoliation hailed the milestone of 2D material, so called Graphene [46, 47] that illustrates the structure of a two dimensional through a thickness less than 1 nm. The unique structure of Graphene (**Figure 2(a)**) illustrates outstanding performance such as extremely high carrier mobility (15,000 cm^2/VS) high thermal conductivity (5300 W/m.K) and high transmittance (97.7%) [48]. Those outstanding performance allures substantial attention on graphene for opening up a responsible fields in Physics (Fermi Dirac), and chemistry with many scientific publications. The electrical, optical and magnetic properties of graphene and its 2D nature has good current integration in the circuit technology, however it limits its application where the electronic band gap is fundamental in optoelectronics. The absence of band gap in graphene provides little ability for cutting off

http://dx.doi.org/10.5772/intechopen.72295

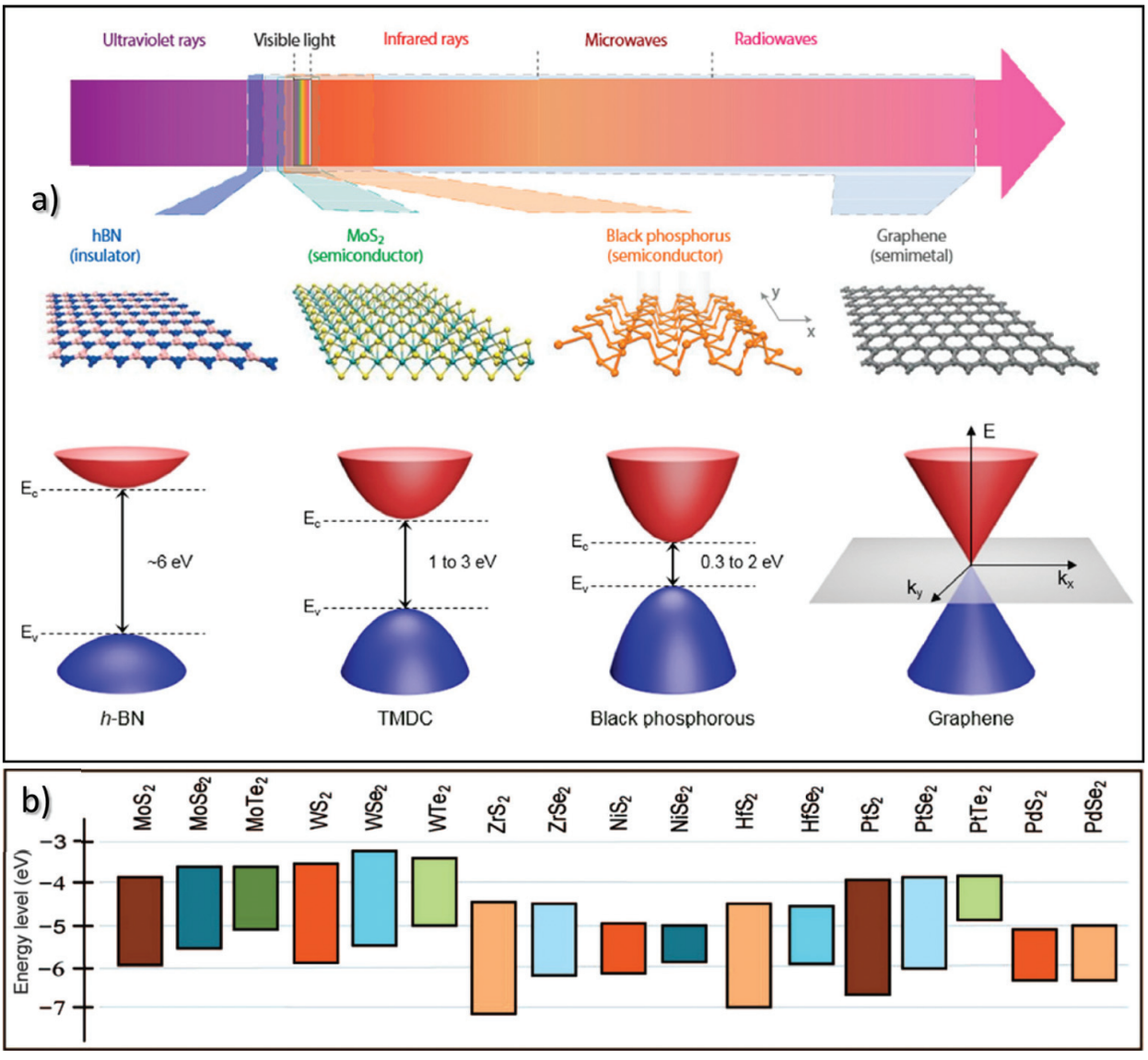

Figure 2. (a) 2D TMDC materials sweeping the energetic region of the electromagnetic spectrum. (b) Energy spectrum of various two-dimensional (2D) materials and their atomic crystal. Adapted from Kourosh et al. [8], Xia et al. [44], Lee et al. [15].

the current while negative bias is applied and it is incapable for exciton disassociation like semiconductors [49]. Now a days the interest for science is extended to other 2D engineering with physical and chemical modifications to introduce novel performances.

Therefore this urges scientists to find out other 2D materials like graphene analogue boron nitrate (BN), transition metal oxide (TMO-like titanium oxide or perovskite), transition metal dichalcogenides (TMDCs) and V-VI/IV-VI compounds naturally have a band gap [50–52]. TMDCs are the elements of the periodic table having a combination (**Table 1**) of two elements with the chemical formula of MX_2: a transitional metal:M, of groups 4–10, and chalcogens:X such as 15 sulfur:S, selenium:Se or tellurium:Te. A single layer TMDCs similar in atomic thicknesses have one layer of atoms that are not comprised as graphene but a planar layer

Graphene family	Graphene	hBN 'White graphene'	BCN	Fluorographene	Graphene oxide
2D chalcogenides	MoS_2, WS_2, $MoSe_2$, WSe_2	Semiconducting dichalcogenides: $MoTe_2$, WTe_2,ZrS_2,$ZrSe_2$ and so on		Metallic dichalcogenides: $NbSe_2$, NbS_2,TaS_2, TiS_2, $NiSe_2$ and so on	
				Layered semiconductors: GaSe, GaTe, InSe, Bi_2Se_3 and so on	
2D oxides	Micas, BSCCO	MoO_3, WO_3		Perovskite – type: $LaNb_2O_7$, $(Ca,Sr)_2Nb_3O_{10}$, $Bi_4Ti_3O_{12}$, $Ca_2Ta_2TiO_{10}$ and so on	Hydroxides: $Ni(OH)_2$, $Eu(OH)_2$ and so on
	Layered Cu oxides	TiO_2, MnO_2, V_2O_5, TaO_3, RuO_2 and so on			Others

Table 1. Current 2D library. Adapted from Geim and Grigorieva [56].

TMDCs involve a metal atom layer sandwiched between layers of chalcogen atoms. They are strongly held together by covalent bonding and the layers are feebly bound together with van der Waals forces allowing it to separate in the bulk sheets. The layered materials combination of Transition metals and Chalcogen family (**Table 1**) have almost 40 different types of TMDCs crystal phases. The different chemical nature of metal and chalcogenide atoms makes the sublattices inequivalent, producing a band gap.

The importance of band-gap engineering in the semiconducting nature of TMDCs is crucial for their potential use in photovoltaic/−catalytic applications, as the ability to tune the material to the correct spectrum or to particular donor/acceptor states in a system is vital in such applications [53, 54] (electronic & photonic). Unlike graphene the semiconducting TMDCs are with a band gap varying from 1 to 3 eV and the band gap (**Figure 2(b)** energy levels of semiconducting TMDCs are sized by changing the number of layers [27]. The TMDCs research was just at their beginning in recent years that built the foundations having a very rapid advances in the scientific field of 2D TMDCs. Obviously, all these methods which effort on gapless graphene are switched for its use on TMDCs. In 2011 with the help of quantum confinement on electronic structure [55], the indirect band gap of bulk TMDCs materials chances to direct band gap in 2D TMDC material of single layer for the coupling of spin and valley physics. The effect of strain allow TMDCs to be a promising use in transistors, optoelectronic and valleytronic devices. The predicted research of the few to monolayer TMDCs focus on identified unique compounds of the TMDCs [7, 56, 57] like MoS_2, $MoSe_2$ & WS_2 etc. exhibit a direct band gap and are of specific interest for new kinds of optoelectronic devices and the bulk crystals are indirect band gap semiconductors.

4. Photodetector technologies and performance

A photo-detector is a key principle device that rely in detecting the process by which light is converted into electrical signals by absorbing the photons [58]. The general action of a photo-detector comprises fundamentally three process, carrier generation, carrier transport and extraction of carriers as terminal output signal current. The schematics of the 2D photo-detectors are shown in **Figure 3(a)**. The fundamental principle of the photo-detector has 3 different stages as Light harvest, photocarrier (e-h) separation and charge transport. It is thus more advantages in the Image defining areas, display technology, networking devices, opto-electronic sensors, and fundamental science applications.

Different mechanisms used in the photodetectors have been identified in literature [59–61] which are crucial process in processing alterations of absorbed photos into an electrical charge. The several possible mechanisms exists, these effects are: photoconductive *(PCE)*, photovoltaic *(PVE)* and photo-thermoelectric *(PTE)* that are discussed below.

4.1. Photoconductive effect (PCE)

This effect is based on the absorption of a photon by a material results in a generation, which can enhance the electrical conductance of the 2D materials [62]. In dark when the device was under an applied bias there will be small current between the two electrodes (without illumination) **Figure 3(b)**. In light when the device was exposed to light photons electron-hole pairs are generated with a higher energy than the band gap. The drift in the electron and holes in different directions lead to an increase in current (I_{photo}) between the metal leads. This photo

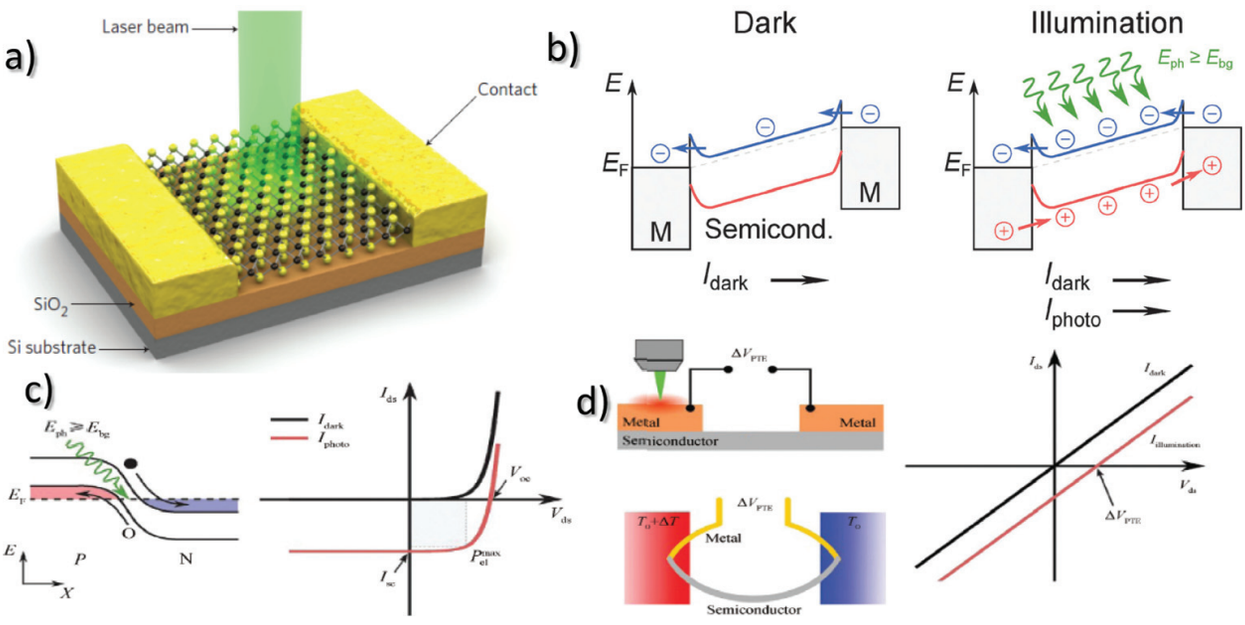

Figure 3. (a) Schematic illustration of 2D photodetector device fabricated on SiO_2/Si substrate. (b) Schematic of the photoconductive effect: in the dark and under illumination. (c) Schematic of the photovoltaic effect: band alignment in a PN junction and I-V curves in the dark & under illumination. (d) Schematic of the photo-thermoelectric effect: the thermal circuit corresponding to the field-effect transistor device and I_{ds}–V_{ds} characteristics in the dark & under illumination. Adapted from Koppens et al. [59], Buscema et al. [66].

generated current increased the conductivity of the device. Due to the large difference between the electron and hole motilities it is important to study the transit time (T) between the electron and holes [63]

$$T_{transit} = \frac{L^2}{\mu V_{ds}} \tag{2}$$

where L, V_{ds} and μ have their regular notations. Many electrons can take part in the photocurrent before whole extraction or recombination which generates the photoconductive gain (G).

4.2. Photovoltaic effect (PVE)

This effect is based on the device when exposed to light and generating voltage. This novel quantum effect for photons for its excitation of an electron hole (e-h) pair parted by an internal electric field which contributes to the photocurrent [64]. Some interface can built the internal electric field, such as Schottky barrier or a PN Junction as shown in **Figure 3(c)**. In dark the detector exhibits nonlinear I-V properties the PN junction is formed, $I_{ds}\ \alpha$ exp. $V_{ds} - 1$ as I_{ds} is exponential with the V_{ds}. When the device is under illumination the photo generated electron-hole pairs can be separated by internal electric field without external voltage leading to a large photocurrent. When the device was under illumination and reverse bias, the photogenerated carriers are wiped out in opposite directions with an increase in the reverse current and the photons energy can be converted into electrical energy by the photovoltaic effect. The voltage ΔV in the process of G-Au interface can be described as:

$$\Delta V = \phi_M - \phi_G - \Delta E_F \ + \text{sgn}\left(V_{gs} - V_{gs}^{Dirac}\right)\hbar v_F \quad \sqrt{\pi\alpha}\sqrt{V_{gs} - V_{gs}^{Dirac}} \tag{3}$$

where φ_M is the work function of metal and φ_G is the work function of graphene; ΔE_F is the shift of the Fermi level of graphene by doping; V_{gs}: gate bias; V_{gs}^{Dirac}: gate bias in electrical neutral point; $\alpha = 7.2 \times 10^{10}\ cm^{-2}\ V^{-1}$ is the carrier concentration with 300 nm SiO_2; $\hbar vF = 5.52$ eVÅ. A bias voltage (external) is to be applied to improve the performance of the device to extract the charge carriers and use the phenomenon of photoelectric effect. The photocurrent can be described in an expanded area in the whole device by applying an external bias voltage that is given by [62, 65]:

$$I_{Ph} = AVe\mu\Delta n \tag{4}$$

the symbols have their usual meaning as the cross section (A), the applied voltage (V), charge (e), the mobility (μ) and the carrier density (Δn). This mechanism can offer great internal gain, which means that the device can detect with extremely low power.

4.3. Photo thermoelectric (PTE) effect

This effect is based on the thermoelectric effect caused by light illumination. When the light energy get absorbed it is sensed by Thermal detectors and the temperature gets raised [66]. **Figure 3(d)** shows the light induced heating leads to a temperature gradient through a

semiconducting channel. Due to Seebeck effect the two ends of the semiconducting channel has a temperature difference ΔT that can convert into a voltage difference ΔV = S. ΔT where ΔV is linearly proportional to ΔT.

Graphene is extensively studied with this mechanism and later the MoS_2 photo-detectors [66–70] having thermoelectric effect by Buscema et al. [66] on the MoS_2 monolayer. The photoinduced current is developed with 750 nm photo source that is less than the band gap of monolayer that is caused by the heating the local junctions between MoS_2 and Gold. The temperature difference between the junctions is due to the absorption of light, creates a generation of PTE current and the voltage difference (ΔV_{PTE}) at the edge of the metal contacts is given by [71]:

$$\Delta V_{PTE} = (\text{S semiconductor} : MoS_2 - \text{S metal} : \text{TiAu})\Delta T \approx \text{S semiconductor} : MoS_2 \Delta T \quad (5)$$

where S is the Seebeck coefficient and ΔT is the difference of temperature (Heated gold electrode & MoS_2) [72]

$$S = \frac{\pi^2 k_B^2 T}{3e} \cdot \frac{dln\,(\sigma(E))}{dE} \,|\, E = E_F \quad (6)$$

where e; the electron charge, k_B; Boltzmann constant, σ(E) is the conductivity, E_F the Fermi energy and T is the temperature.

4.4. Photo-device performance

The key terms of merit that are at high priority to characterize and assess the photo-detector performances are as listed below:

Photo gain (G_{ph})

Photo response time:

On/Off ratio

External Quantum Efficiency (EQE) and

Internal Quantum Efficiency (IQE)

Photoresponsivity (R_λ) and

Detectivity (D)

Photo gain:

The ratio of the detected charge carriers per single incident photons, given by G_{ph} and is defined by [63]

$$G_{ph} = \frac{\tau_{tr}}{\tau_{transit}} = \frac{\tau_{tr} \mu V_{bias}}{L^2} \quad (7)$$

Here, τ_{tr} is the life time of the charge carriers, $\tau_{transit}$ is the drift transit time, μ is the mobility of the charges and L is the source—drain separation distance.

Photoresponse time:

In the ON state from dark, the time required for the current change until saturation is considered. This time varies from μs to minutes in different 2D materials and related devices that can limit the application of the photo-detector.

On/Off ratio:

The ON/OFF in the photodetector is the fraction of the current with light ON and the current (I) in Dark. It is not very similar to the device ON-OFF ratio in the other FET devices.

External Quantum Efficiency (EQE):

In order to produce the photocurrent I_{ph} the fraction of the extracted free charge carriers to the photo flux φ_{in} collected at a given energy E_{ph} is the External Quantum Efficiency, defined by [73]:

$$\mathrm{EQE} = \frac{\mathrm{I_{ph}}}{e\phi_{\mathrm{in}}} = \frac{h\nu}{\mathrm{e}}\frac{\mathrm{I_{ph}}}{\mathrm{P_{in}}} \tag{8}$$

where P_{in} is the incident power.

Internal Quantum Efficiency (IQE):

In order to produce the photocurrent I_{ph} the sharp ratio of the number of free charge carriers collected is slightly different from external. The energy E_{ph} is given by the absorbed count of photons is the External Quantum Efficiency, described by [73]:

$$\mathrm{IQE} = \frac{\mathrm{I_{ph}}}{\mathrm{e}\varphi_{\mathrm{in}}\mathrm{A_{abs}}} = \frac{\mathrm{h}\nu}{\mathrm{e}}\frac{\mathrm{I_{ph}}}{\mathrm{P_{in}}\mathrm{A_{abs}}} \tag{9}$$

here A_{abs} mentions the fraction of absorption.

Photoresponsivity:

Photoresponsivity is defined by R_λ on the effective area of the photocurrent I_{ph} generated per unit incident power P of the photo-detector (S) [5, 74, 75]:

$$\frac{\mathrm{I_{ph}}}{\mathrm{P_{in}}} = \frac{\mathrm{I_{ph}}}{\mathrm{P} \times \mathrm{S}} = \frac{\eta\ \mathrm{q}}{\mathrm{hv}} \tag{10}$$

where η; is quantum efficiency, and the responsivity is termed as [67]

$$\mathrm{R} = \frac{\eta\lambda q}{\mathrm{hc}} = \frac{\eta\lambda\ (\mu m)}{1.24}\ \left(\frac{\mathrm{A}}{\mathrm{W}}\right) \tag{11}$$

where λ is the incident wavelength.

Quantum efficiency:

Quantum efficiency (QE) (η%) *of a photodetector* is the ratio of the electron generation rate to the photon incidence rate. QE is connected to the responsivity of the photo detector by the below equation [58, 76]

$$\eta = \frac{\frac{I_{ph}}{q}}{\frac{P_{inc}}{hv}} = \frac{I_{ph}}{q} \cdot \frac{hv}{P_{inc}} \tag{12}$$

Detectivity:

The ability of the Detector D represents the detector to distinguish between signal/noise [77, 78]:

$$D = \frac{R_\lambda \sqrt{A}}{\sqrt{2eI_{dark}}} \tag{13}$$

where I_{dark} is the dark current.

In 1873 the birth of photo-detectors was traced in the discovery of photoconduction of selenium [79] and was first fabricated in 2009. The Graphene as the prototype 2D material started working without any bias voltage showing steady state photo-response up to a frequency of 40 GHz. The photodetectors of graphene have broader absorption spectrum, fast response time and a carrier mobility that are energetic elements and the exfoliated graphene has the highest photoresponsivity (6.1 mA/W) and weak absorbance which is a limitation for exfoliated graphene photo-detectors [80]. Now a days, the 2D transition metal dichalcogenide semiconductors (TMDCs) have successfully fabricated for larger absorption that has raised their limitation to improve the performance of photodetector. The monolayer exfoliated MoS_2 has a photoresponsivity of 880 A/W at 561 nm and the energy band gap of TMDCs layers is tuned between direct and indirect which is crucial in designing efficient photo-detectors [81].

5. 2D photo devices

2D material devices are fabricated with the contacts and are patterned by means of physical mask & lithography (both electron beam and optical lithography) In addition, metallization, lift off process and vacuum annealing are the hardcore essential steps for a final material device fabrication. Extensive discussion is carried on the experimental techniques of material device fabrication by using physical mask and optical lithography respectively. The three parameters like metal evaporation, lift off and vacuum annealing are necessarily of more interest to be discussed.

5.1. Fabrication

Physical mask: The physical stencil mask is the modest device fabrication method that is fast and clean. The device performance is fictional with the lithography process having good

transparency in the 2D material homo-structures. The fabrication of the device is carried with physical mask and prepared first on silicon substrate. The precised mask is aligned and stuck tight on the substrate by making contacts having the metals get evaporated. The 2D device is at last fabricated by eliminating the mask.

Lithography: Lithography is an effective process used in the fabrication of the device and is a planning tool to prepare the device contacts and to overcome some of the problems in the application of 2D materials. Electron beam lithography and Optical lithography differ technically but sounds good in the applications of universal devices. The E-Beam lithography can be of more advantage in device application as the precision can reach nm scale and the design of the mask is done with requirement of the samples. **Figure 4(a)** & **(b)** depicts the schematic of electron beam lithography and at first the resist is spin coated onto the substrate (for optical lithography) or sample (for electron beam lithography) and dried in a hot plate. Secondly, the UV light or electron beam exposes the patterns of the mask and starts to change the resist properties. The pattern obtained is developed after the exposure. Thirdly, the patterned samples are deposited with the metals (Ti/Au), and finally the metals/resist is removed in the lift off process to advance the device.

Metal evaporation: The metals get evaporated by arranging the devices and substrates, alignment of stencil mark or the lithography by using gold, titanium and carbon and chrome metals. The development compute the process to have normal contacts, evaporation of 5 nm Cr-Ti followed by 70 nm Au with careful consideration.

Lift off (only made by lithography): Lift off is a simple, easy method for exposing a pattern into photoresist depositing a thin film and washing to leave behind only the film in the patterned area. The resist is lifted off the substrate on the top of the metal that gets evaporated and lithography is done. This process is carried in a hot acetone of temperature around 50–60°C, in 2 h time the metal on the top gets lifted off after the resist gets dissolved.

Annealing (only made by lithography): This is the important process that is very important to fabricate the devices. It is important to remove the residual of resist/impurities in vacuum. In order to maintain good contact among the sample and the metal its crucial to input certain

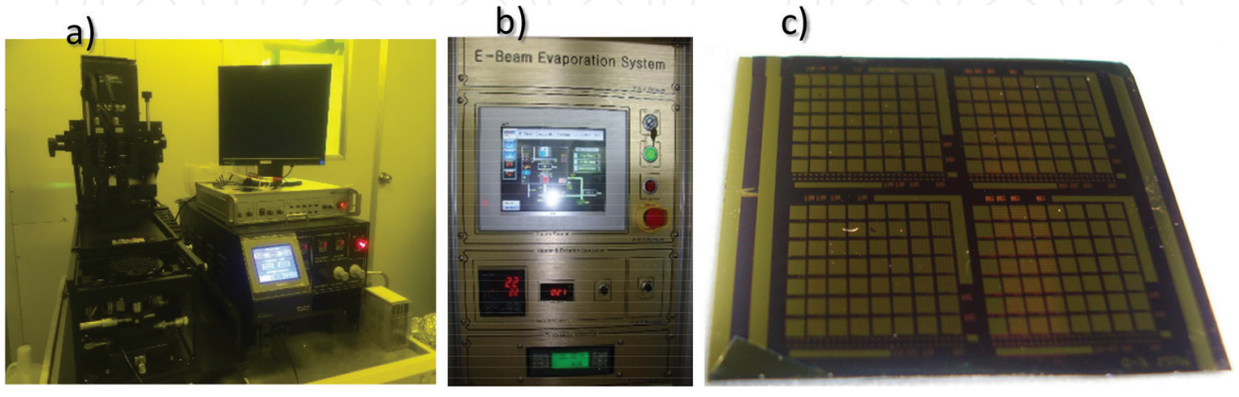

Figure 4. (a) Optical lithography. (b) E-Beam system. (c) Schematic of 2D final device fabrication with grids as a shadow mask with SiO_2 dielectric and Ti/Au electrodes.

device current to remove critical contaminants in the optimization of metal:sample interface, which is the most critical step in device fabrication (**Figure 4(c)**).

The different TMDC devices on 2D layered semiconductors is comprehensively reviewed and discussed about the photodetection applications beyond graphene. **Figure 5** [17] shows the timeline development of the applications of graphene and other 2D layered semiconductors in photodetectors based on different principles.

Most of the fabricated single/few layer TMDC FETs exhibits an n-type semi conducting behavior which might approach the saturation current. The threshold voltage indicates the natural n-type doping that arises due to the impurities like halogen (Br/Cl) atom that likely to replace S atoms. The gradual increase of the concentration of the electrons of TMDCs giving n-type doping results. The field effect device mobility of the single/few layer devices can be estimated with the below equation [82]

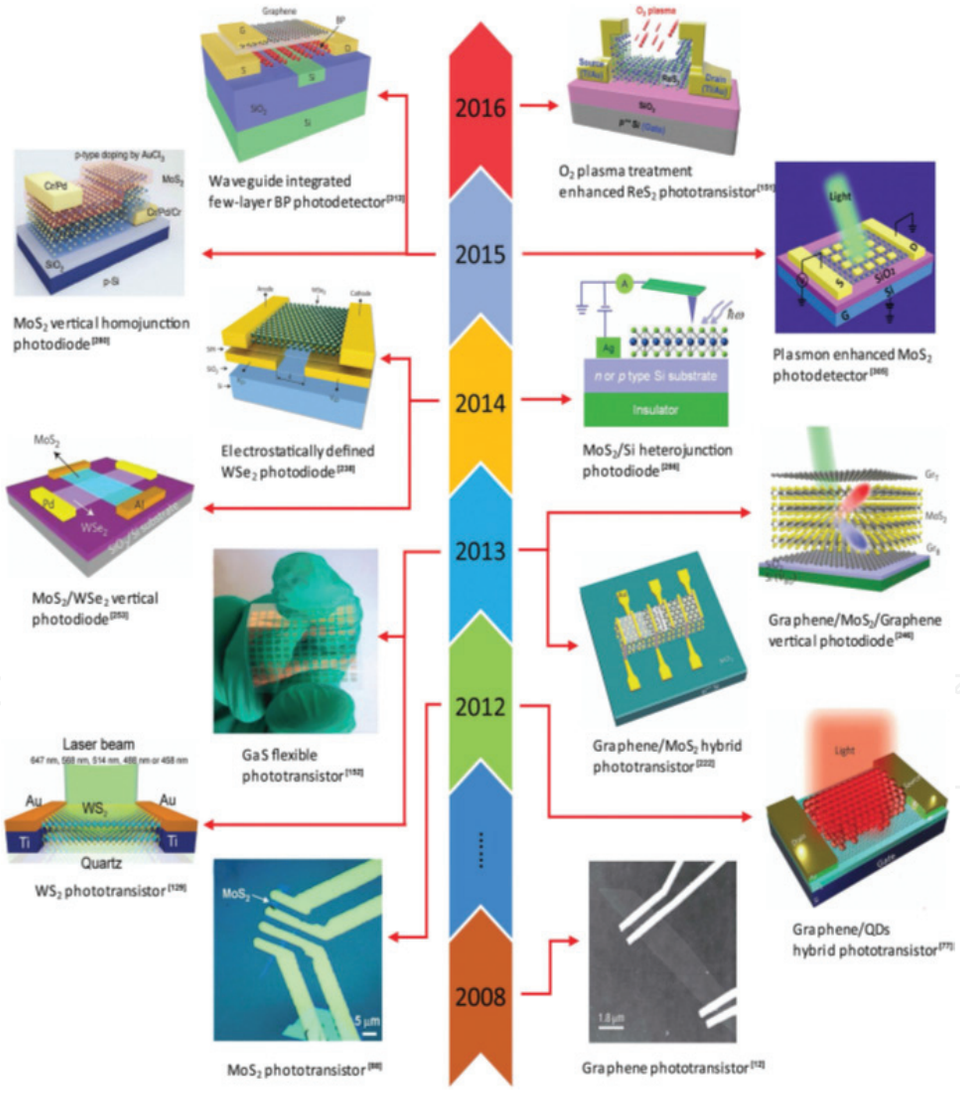

Figure 5. Timeline showing the development of the applications of graphene and other 2D layered semiconductors in photodetectors based on different principles. Adapted from Xie et al. [17].

$$\mu = \left(\frac{L}{WC_{ox}V_{ds}}\right)\left(\frac{\partial I_{ds}}{\partial V_{gs}}\right) \tag{14}$$

where L, W, C_{ox} have their usual meaning like the device channel length, width and gate capacitance per unit area of 1.15×10^{-8} F/cm^2. It is well known that the carrier mobility of semiconductors tend to decrease with increasing band gap. The electron mobility trend from III to V compounds reduces from 77,000 cm^2/VS for the narrow band gap to 3000 cm^2/VS for the wider band gap [83]. The gapless graphene show very high mobility of up to 200,000 cm^2/VS [84]. The electron mobilities among 2D materials beyond graphene shows a high field effect mobility μ_{eff} > 100 cm^2/VS for MoS_2 and an average mobility of ~50 cm^2/VS/~100 cm^2/VS for single/bulk $MoSe_2$ [85, 86]. With various 2D blocks in hands the key parameters provide large collection of mobility with strong light absorption in literature [87, 88] has transfer (I_{ds} – V_{gs}) and output (I_{ds} – V_{ds}) characteristics of different TMDC synthesis.

5.2. Photodetector parameters

Choosing to study the optoelectronic properties of the semiconducting two dimensional materials like the TMDCs family consisting of transition metal dichalcogenides have shown a great deal of attention towards strong light-matter interaction for optoelectronic applications. The selection of the photodetector is based on the wavelength of light detected and the basic photodetectors are semiconducting optical devices that adapt the incident light to an electrical light that is focused as photocurrent [89]

$$I_{ph} = BP^m \tag{15}$$

where I_{Ph} is the photocurrent, B is a constant, m is an exponent determining the photoconduction mechanism and P is the illumination intensity. In order to understand the photodetection high responsivity is required and essential for its potential application in TMDCs materials which is a good parameter for the performance of an improved photodetector. It is defined by [90]

$$R_\lambda = \frac{I_P}{P_{light}} \tag{16}$$

where $I_P = I_{illumination} - I_{dark}$ and P_{light} is the power of incident light.

The detector response should be great at the detected wavelength and different laser beams are used at several optical power and applied gate voltage. The laser beams are chosen with a laser wavelength of 532 nm is used in producing a photocurrent by focusing the light with a spot diameter less than 1 μm. The I & V parameters tend to increase with the increasing light intensity that strongly suggest the photocarriers having electric field separated at the interface of 2D and Si. To know the potential application of TMDC materials in photodetection, high responsivity in various 2D TMDCs have been used for high performance photo-detectors such as, MoS_2, $MoSe_2$, WS_2, $MoTe_2$, & $ReSe_2$ and so on [91–94]. These TMDCs in **Figure 6** can provide additional advantages over graphene based photodetectors that have larger photoresponsivity

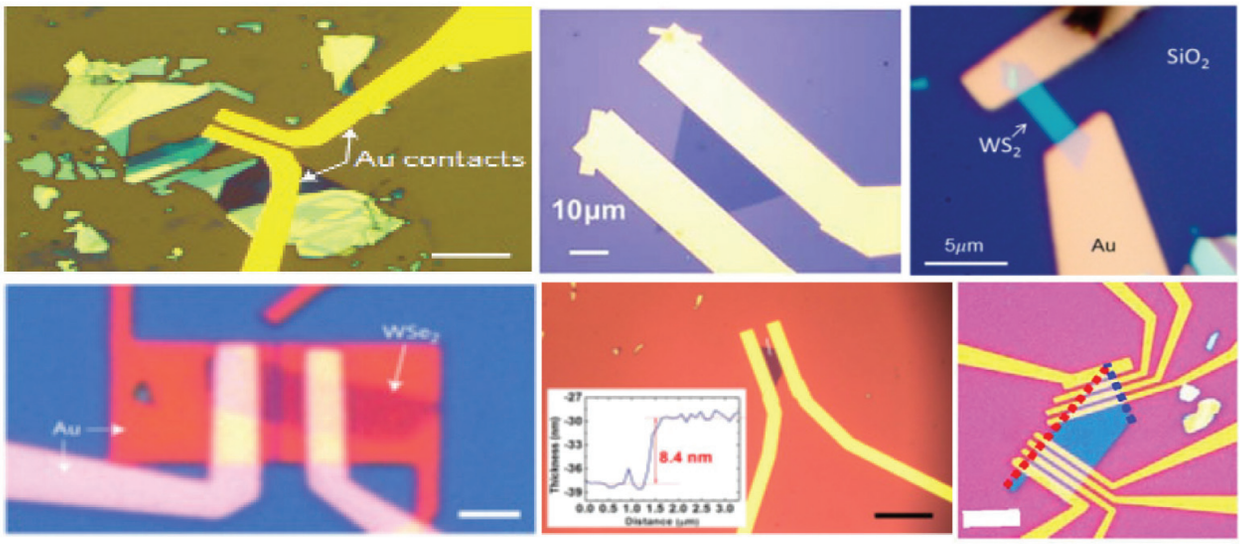

Figure 6. Optical and AFM images of different 2D devices gated using a degenerately doped silicon substrate with two gold contacts. Adapted from Lopez-Sanchez et al. [23], Xia et al. [101], Liu et al. [18], Baugher et al. [19], Huang et al. [20], Liu et al. [112].

of 10 mA/W to date in pure graphene photo-detector in visible region. Compared to classical direct band gap semiconductors TMDCs are more advantages due to its transparency, easy processing, and flexibility has ability to detect light at different wavelengths by tuning their optical gap with various number of layers.

Graphene cannot be used as a competent photo-detector, with great dark current & small absorption and photoresponsivity. MoS_2 is a representative member of the transition metal dichalcogenide (TMDC) family that consists of two-dimensional material planar sheets that stack on each other together using weak van der Waals interlayer interactions. MoS_2 is a said to replace the graphene having promising alternative properties to enhance photocurrent response because it has a band gap of 1.8 eV and high mobility of above 100 cm^2/VS [95]. MoS_2 based photodetectors are of two kinds; (a) direct band gap on single-layer MoS_2 (b) indirect band gap on few-layer MoS_2. In 2011 the first photo-detector is based on single layer MoS_2 was fabricated and developed [32], having a photoresponse of 7.5 mA/W, response time of 50 ms which can measure 750 nm light that is comparable to graphene based photo-detectors. As in **Figure 7** in ambient condition Lopez-Sanchez with his group [24] developed a device based on monolayer MoS_2 yielding a highest photoresponsivity of 880 A/W and on the other hand in high vacuum condition a CVD monolayer MoS_2 based photo-detector arrive a photoresponse and photogain limiting to 2200 and 5000 A/W respectively [96]. This implies that the environment has a great influence on both the electronic and the optoelectronic properties. Beside single layer MoS_2, few-layer MoS_2 photodetectors have unique properties, such as large absorption, band gap reduction and lower photoresponsivity than single layer photodetectors. The reduction in responsivity is caused by the indirect band gap and the trap states dominate the photodetection mechanism in few layer MoS_2. In 2012 W. Choi et al. [20] fabricated a photo-detector based on multilayer MoS_2 having a wide (~900 nm) spectral response with a high photoresponse (>100 mA/W) and photo-detector based on a double layer

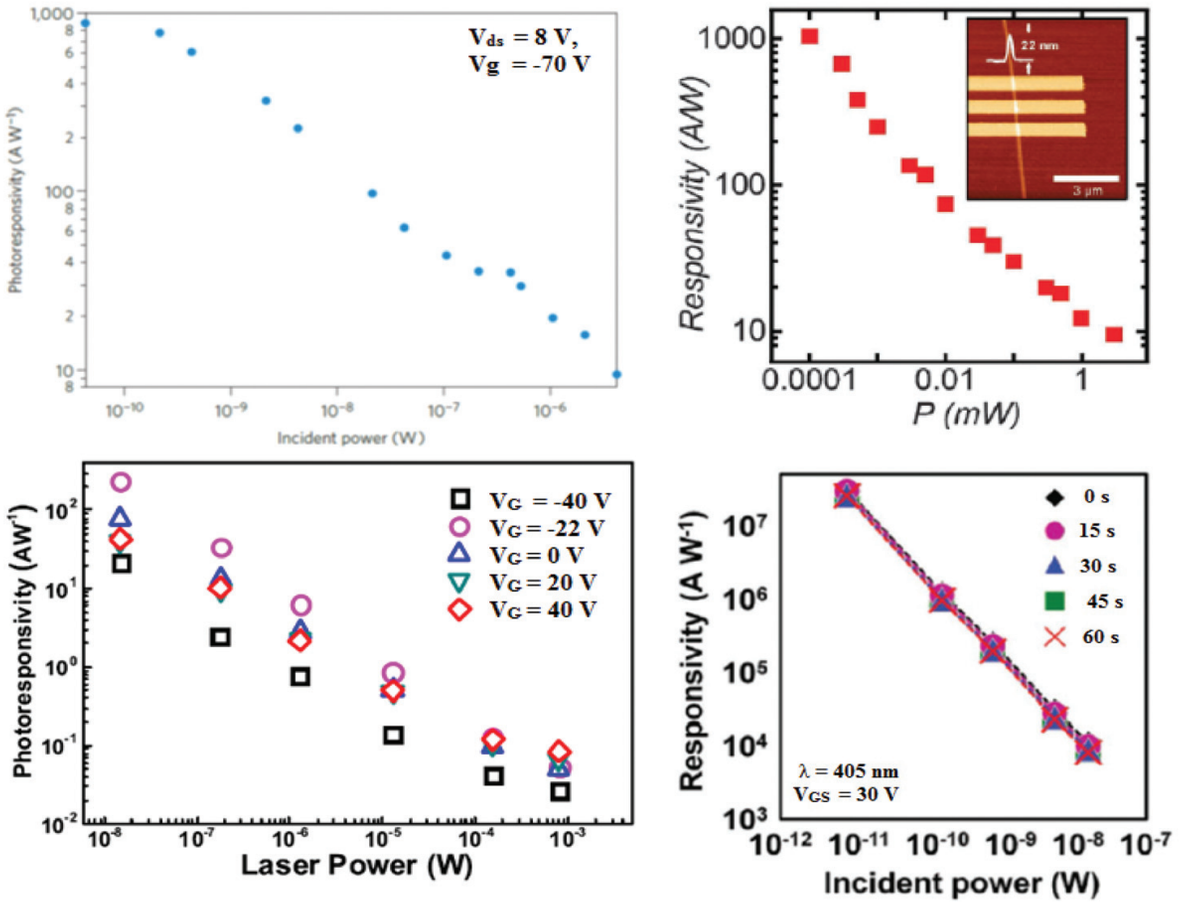

Figure 7. Photoresponsivity of 2D TMDC devices under illumination wavelength. The TMDC devices shows an increasing response of the photodetectors used for a high broad range of wavelengths. Adapted from Lopez-Sanchez et al. [23], Ko et al. [21], Shim et al. [113], Buscema et al. [66].

MoS_2 device giving a faster photoresponse of (~110 μs; decay ~70 μs; rise) 570 mA/W of photoresponsivity of 10 V and had high thermal stability In a different study top-gated photodetectors depending on three different layers like single: double: triple 2D MoS_2 [33–35] are compared and there outcomes indicate that the triple-layer device exhibits a very improved detection with red source, and the others like double-layers and single layer were more valuable for an energy of higher green detection. Since decade's significant advances have been achieved to synthesize large continues films or triangular flakes or hexagonal flakes on different substrates [57, 97–99]. Like MoS_2 the properties of monolayer $MoSe_2$ exhibits a direct band gap of 1.6 eV and changes into indirect band gap of 1.1 eV for bulk or multilayer $MoSe_2$. $MoSe_2$ Photodetectors based on single/multilayer devices shows a remarkable light response, speed response (15 ms–8 s) remains too low for practical applications [100, 101].

The CVD grown $MoSe_2$ Photodetectors exhibit high photoresponsivity between 0.26 and 13 mA/W [101] and Duan et al. [102] demonstrated the epitaxial growth of $MoSe_2/MoS_2$ heterojunctions which showed a pronounced photoresponse characteristics. The exfoliated flake based photodetector shows a responsivity of 10^6 was transferred on Ti electrodes up to 97.1 A/W and the heterojunction photodetector like $Gr/MoSe_2/Si$ display a photoresponse in

the wide range of 350–1310 nm having an extreme fast response speed of 270 ns. The $MoSe_2$ devices show a fast response speed within a few tens of milliseconds for high performance optoelectronic devices. Among the 2D materials the tungsten disulfate (WS_2) has been investigated for its use in photodetectors under the influence of gaseous environment. Recently Huo and his group [81, 103] carried the measurements under low excitation powers and the photoresponsivity of the devices ranges from 13 A/W in vacuum to 884 A/W in NH_3 atmosphere. The WS_2 photodetector has good improvement in the responsively and sensing performances. Besides WS_2, tungsten diselenide (WSe_2) can also be used as sensing material for photodetectors and a high responsively of 180 and 30 A/W is reported on the influence of metal electrodes on photoresponse [104, 105].

The $MoTe_2$ 2D material shows the electrical properties of a phototransistor based on mechanically exfoliated few layer $MoTe_2$ device that reached a responsivity of 2560 A/W [106]. Xu and coworkers successfully isolated the single and few layer HfS_2 flakes by mechanical exfoliation that has an indirect band gap of 2 eV shows a responsivity of $\sim$ 890 A/W [107]. $ReSe_2$ based photodevices on single layer reports an extraordinary responsivity of 95 A/W with a fast response times on the order of tens of ms. ReS_2 has a direct band gap of 1.5 eV and the CVD grown and exfoliated few layer ReS_2 shows a responsivities ranging from 16.14 A/W to 8.86×10^5 A/W [108] with a response time of several ms to hundreds of s. Few layer ReS_2 based transistors under the oxygen plasma treatment can advance the optoelectronic properties with a maximum responsivity of 16 A/W, 88,600 A/W & 2.5×10^7 A/W [109–112] and a response time of several tens of seconds. The GaSe based devices show a photoresponse of 2.8 A/W and a response time of 0.02 s while GaS based devices show responsivities of up to 4.2 A/W and 19.2 A/W and the devices with GaTe exhibit increased responsivities between 274.3 A/W and 10^4 A/W having a response speed down to several ms [113]. The GaSe and GaS has photoresponsivity of 4 A/W on flexible substrates in the UV Blue region and the direct band gap GaTe and In_2Se_3 exhibits large responsivities of 1×10^4 A/W at short light illumination and response time varies from ms to s [114–116]. A thicker InSe flake has a great photoresponse of 160 A/W and a fast response speed of few seconds that indicates a great influence of trap states. SnS_2 flakes has a great attention used in photodetectors & transistors synthesized by the exfoliation method and CVD grown flakes can reach up to a high responsivity of 8 mA/W with a response time of 5 ms [117]. To enhance the performance of photodetector devices at faster response times in the absence of gain and responsivity on the order of mA/W can achieve the highest sensitivity ($D^* \geq 7.7 \times 10^{11}$ jones) in TMDC photodetectors [17]. Combining the critical parameters presented in table [17] like photoresponse time, Detectivity and EQE a high speed and highly sensitive photodetector could be realized by stacking of TMDCs and other two dimensional materials. The photodetectors on different semiconducting TMDCs beyond MoWSeS (MoS_2:R_{ph} = 0.57 A/W, GaS: R_{ph} = 19 A/W, GaSe: R_{ph} = 2.8 A/W, In_2Se_3: R_{ph} = 3.95 A/W) materials have their use in the flexible electronics of noble metals (PdS_2, PtS_2…) and the early transition metals (e.g. TiS_2, ZrS_2, HfS_2…) [118–122]. The growth of the devices between their in-plane and out-of-plane modes have recently been discovered as nanodiscs. These scientific discoveries are a frontline portion of the technological evolving field and these 2D materials beyond graphene are blooming with new devices based on MoWSeS materials, and investigation on the layered TMDCs research is still in early stages.

6. Conclusions

This chapter is discussed on the Photodetectors based on 2D Transition metal Dichalcogenides (TMDCs) that are rapidly established themselves as fascinating blocks for optoelectronics focusing on the photoresponsivity. After the graphene discovery in 2004 thin film TMDCs are used in the demonstration of the novel nanoelectronic and optoelectronic devices that are becoming more eminent. The topdown & bottomup synthesis routes including Chemical vapor deposition, hydrothermal method, electrical and mechanical exfoliation methods are the promising methods to improve photocurrent response and discussion is carried on 2D TMDC materials for a strategy to obtain large area with controlled thickness. The 2D TMDCs with wide range of material properties can exhibit an ironic physical behavior extending from an insulator to a narrow gap semiconductor to a semi metal or metal. The 2D TMDC semiconductors can have strong interaction with light and enhance the photon absorption with the number of layers and evident with the band gap structures to create electron hole creation in the merit of photodetection. The large band gap of TMDCs has higher carrier lifetimes allowing them as a promising candidate for high sensitivity photodetectors. The direct band gap semiconductors are suitable for application in optoelectronic devices generating electron-hole pair with high absorption coefficient for effective photoresponse characteristics. The key principle in the photo detection is explained and several different mechanism have been discussed to enhance the photodetection efficiency. The theoretical key parameters of photo performance is well explained to improve the light-matter interaction. The phototransistor device preparation is shown and the Phototransistor devices based on TMDCs monolayer/multilayers show and report the device photoresponsivity reaching 880–2570 A/W and having a high photodetectivity under the light intensity. The improvement of TMDC photodetectors performance like the parameter photoresponsivity is explained clearly in all the different TMDC materials which is favorable for photodetection current that can greatly enhance the photoresponse speed. The predictions of 2D materials in the commercialization depends on the ability to offer at large scale depend not only on their performance but also on the ability low cost integration to the existing photonic and electronic devices.

Acknowledgements

The authors would like to thank the financial support from National Research Foundation of Korea (grant NRF – **2017035339**).

Author details

Inturu Omkaram*, Young Ki Hong and Sunkook Kim*

*Address all correspondence to: inturuomkar@gmail.com and kimskcnt@gmail.com

School of Advanced Materials Sciences and Engineering, Sungkyunkwan University, Gyeong-gi, South Korea

References

[1] Huang X, Yin ZY, Wu SX, Qi XY, He QY, Zhang QC, Yan QY, Boey F, Zhang H. Graphene-based materials: Synthesis, characterization, properties and applications. Small. 2011;**7**:1876-1902

[2] Sze SM, Ng KK. Physics of Semiconductor Devices. 3rd ed. United States of America: Wiley; 2007

[3] Kolobov AV, Tominaga J. Two-Dimensional Transition-Metal Dichalcogenides. Switzerland: Springer; 2016. p. 239

[4] Jiang HJ. Chemical preparation of graphene-based nanomaterials and their applications in chemical and biological sensors. Small. 2011;**7**:2413-2427

[5] Koppens FHL, Mueller T, Avouris P, et al. Photodetectors based on graphene, other two-dimensional materials and hybrid systems. Nature Nanotechnology. 2014;**9**(10):780-787

[6] Neto AC, Guinea F, Peres N, Novoselov KS, Geim AK. The electronic properties of graphene. Reviews of Modern Physics. 2009;**81**:109-162

[7] Mak KF, Lee C, Hone J, Shan J, Heinz TF. Atomically thin MoS_2: A new direct-gap semiconductor. Physical Review Letters. 2010;**105**:136805 (1-4)

[8] Kourosh KZ, Jian ZO, Torben D, Michael SS, Martin P, Sally LG. Two-dimensional transition metal dichalcogenides in biosystems. Advanced Functional Materials. 2015; **25**:5086-5099

[9] Wang QH, Kalantar-Zadeh K, Kis A, Coleman JN, Strano MS. Electronics and optoelectronics of two-dimensional transition metal dichalcogenides. Nature Nanotechnology. 2012;**7**:699-712

[10] Bultler SZ, Hollen SM, Cao L, et al. Progress, challenges and opportunities in two-dimensional materials beyond graphene. ACS Nano. 2013;**7**(4):2898-2926

[11] Wang H, Yu L, Lee YH, Shi Y, Hsu A, Chin ML, Li L-J, Dubey M, Kong J, Palacios T. Integrated circuits based on bilayer MoS_2 transistors. Nano Letters. 2012;**12**:4674-4680

[12] Novoselov KS, Castro Neto AH. Two-dimensional crystals-based heterostructures: Materials with tailored properties. Physica Scripta. 2012;**T146**:014006 (6pp)

[13] Zhang W, Zhang P, Su Z, Wei G. Synthesis and sensor applications of MoS_2-based nanocomposites. Nanoscale. 2015;**7**:18364-18378

[14] Shi Y, Li H, Li LJ. Recent advances in controlled synthesis of two dimensional transition metal dichalcogenides via vapour deposition techniques. Chemical Society Reviews. 2015;**44**:2744-2756

[15] Lee JY, Shin J-H, Lee G-H, Lee C-H. Two-dimensional semiconductor optoelectronics based on van der Waals heterostructures. Nanomaterials. 2016;**6**:193-211

[16] Zheng L, Zhongzhu L, Guozhen S. Photodetectors based on two dimensional materials. Journal of Semiconductors. 2016;**37**:091001 (1-11)

[17] Xie C, Mak C, Tao X, Yan F. Photodetectors based on two-dimensional layered materials beyond graphene. Advanced Functional Materials. 2017;**27**:1603886-1603927

[18] Liu X, Hu J, Yue C, Fera ND, Ling Y, Mao Z, Wei J. High performance field-effect transistor based on multilayer tungsten disulfide. ACS Nano. 2014;**8**:10396-10402

[19] Baugher BWH, Churchill HOH, Yang Y, Jarillo-Herrero P. Optoelectronic devices based on electrically tunable p–n diodes in a monolayer dichalcogenide. Nature Nanotechnology. 2014;**9**:262-267

[20] Huang H, Wang J, Hu W, Liao L, Wang P, Wang X, Gong F, Chen Y, Wu G, Luo W. Highly sensitive visible to infrared $MoTe_2$ photodetectors enhanced by the photogating effect. Nanotechnology. 2016;**27**:445201-445208

[21] Ko PJ, Abderrahmane A, Kim N-H, Sandhu A. High-performance near-infrared photodetector based on nano-layered $MoSe_2$. Semiconductor Science and Technology. 2017;**36**: 065015-065022 (8pp)

[22] Jiang FK, Lee GB, Tai YC, et al. A flexible micromachine-based shear-stress sensor array and its application to separation-point detection. Sensors and Actuators A: Physical. 2000;**79**:194-203

[23] Lopez-Sanchez O, Lembke D, Kayci M, Radenovic A, Kis A. Ultrasensitive photodetectors based on monolayer MoS_2. Nature Nanotechnology. 2013;**8**:497-501

[24] Jo S, Ubrig N, Berger H, Kuzmenko AB, Morpurgo AF. Mono- and bilayer WS_2 light-emitting transistors. Nano Letters. 2014;**14**:2019-2025

[25] Bae S, Kim H, Lee Y, Xu XF, Park JS, Zheng Y, Balakrishnan J, Lei T, Kim HR, Song YI, Kim YJ, Kim KS, Ozyilmaz B, Ahn JH, Hong BH, Iijima S. Roll-to-roll production of 30-inch graphene films for transparent electrodes. Nature Nanotechnology. 2010;**5**:574-578

[26] Bonaccorso F, Sun Z, Hasan T, Ferrari AC. Graphene photonics and optoelectronics. Nature Photonics. 2010;**4**:611-622

[27] Splendiani A et al. Emerging photoluminescence in monolayer MoS_2. Nano Letters. 2010;**10**:1271-1275

[28] Sze S. Semiconductor Devices, Physics and Technology. 2nd ed. New York, USA: John Wiley & Sons; 2002

[29] Tran QT, Le TD, Subramanian R, Nae-Eung L. Transparent, stretchable, and rapid-response humidity sensor for body-attachable wearable electronics. Nano Research. 2017;**10**:2021-2033

[30] Wu C, Kim TW, Li F, Guo T. Wearable electricity generators fabricated utilizing transparent electronic textiles based on polyester/Ag nanowires/graphene core–shell nanocomposites. ACS Nano. 2016;**10**(7):6449-6457

[31] Wang X, Yusheng C, Xinlong W, Lei L, Xinhua O, Ziyi G, Hui H. MoS_2 quantum dots with a tunable work function for high-performance organic solar cells. ACS Applied Materials & Interfaces. 2016;**8**(40):26916-26923

[32] Yin Z et al. Single-layer MoS_2 phototransistors. ACS Nano. 2011;**6**:74-80

[33] Kwon J, Hong YK, Han G, Omkaram I, Choi W, Kim S, Yoon Y. Giant photoamplification in indirect-bandgap multilayer MoS_2 phototransistors with local bottom-gate structures. Advanced Materials. 2015;**27**:2224-2230

[34] Lee HS, Min S-W, Chang Y-G, Park MK, Nam T, Kim H, Kim JH, Ryu S, Im S. MoS_2 nanosheet phototransistors with thickness-modulated optical energy gap. Nano Letters. 2012;**12**:3695-3700

[35] Choi W, Cho MY, Konar A, Lee JH, Cha G-B, Hong SC, Kim S, Kim J, Jena D, Joo J, Kim S. High-detectivity multilayer MoS_2 phototransistors with spectral response from ultraviolet to infrared. Advanced Materials. 2012;**24**:5832-5836

[36] Britnell L, Ribeiro R, Eckmann A, Jalil R, Belle B, Mishchenko A, Kim Y-J, Gorbachev R, Georgiou T, Morozov S. Strong light-matter interactions in heterostructures of atomically thin films. Science. 2013;**340**:1311-1314

[37] Geim AK, Novoselov KS. The rise of graphene. Nature Materials. 2007;**6**:183-191

[38] Zheng J, Zhang H, Dong S, Liu Y, Tai Nai C, Suk Shin H, et al. High yield exfoliation of two-dimensional chalcogenides using sodium naphthalenide. Nature Communications. 2014;**5**:2995 (1-7)

[39] Guo X, Wang Y, Wu F, Ni Y, Kokot S. A colorimetric method of analysis for trace amounts of hydrogen peroxide with the use of the nano-properties of molybdenum disulfide. The Analyst. 2015;**140**:1119-1126

[40] Lee YH, Zhang XQ, Zhang W, Chang MT, Lin CT, Chang KD, et al. Synthesis of large-area MoS_2 atomic layers with chemical vapor deposition. Advanced Materials. 2012;**24**: 2320e5

[41] Wilson JA, Yoffe AD. Transition metal dichalcogenides discussion and interpretation of observed optical, electrical, and structural properties. Advances in Physics. 1969;**18**:193-335

[42] Novoselov KS, Jiang D, Schedin F, Booth TJ, Khotkevich VV, Morozov SV, et al. Two-dimensional atomic crystals. Proceedings of the National Academy of Sciences of the United States of America. 2005;**102**:10451-10453

[43] Chalcogenides fill the gap, Nature Materials. 2014;**13**:1073-1073

[44] Xia F, Wang H, Xiao D, Dubey M, Ramasubramaniam A. Two-dimensional material nanophotonics. Nature Photonics. 2014;**8**:899-907

[45] Radisavljevic B, Kis A. Mobility engineering and a metal–insulator transition in monolayer MoS_2. Nature Materials. 2013;**12**:815-820

[46] Novoselov KS, Geim AK, Morozov SV, Jiang D, Zhang Y, Dubonos SV, Grigorieva IV, Firsov AA. Electric field effect in atomically thin carbon films. Science. 2004;**306**(5696):666-669

[47] Tang Q, Zhou Z. Graphene-analogous low-dimensional materials. Progress in Materials Science. 2013;**58**:1244-1315

[48] Fuhrer MS. Graphene: Ribbons piece-by-piece. Nature Materials. 2010;**9**:611-612

[49] Giovannetti G, Khomyakov PA, Brocks G, Kelly PJ, van den Brink J. Substrate-induced band gap in graphene on hexagonal boron nitride: Ab initio density functional calculations. Physical Review B. 2007;**76**:073103

[50] Jariwala D, Sangwan VK, Lauhon LJ, Marks TJ, Hersam MC. Emerging device applications for semiconducting two-dimensional transition metal dichalcogenides. ACS Nano. 2014;**8**:1102-1120

[51] Kuc A, Zibouche N, Heine T. Influence of quantum confinement on the electronic structure of the transition metal sulfide TS_2. Physical Review B. 2011;**83**:245213

[52] Kappera R. Electrical properties and phase engineering of two dimensional MoS_2 [thesis]; United States: The state University of New Jersey; 2015

[53] Tonndorf P, Schmidt R, Böttger P, Zhang X, Börner J, Liebig A, Albrecht M, Kloc C, Gordan O, Zahn DRT, et al. Photoluminescence emission and Raman response of monolayer MoS_2, $MoSe_2$, and WSe_2. Optics Express. 2013;**21**:4908-4916

[54] Andreas P, Thomas M. Optoelectronic devices based on atomically thin transition metal dichalcogenides. Applied Sciences. 2016;**6**:78. DOI: 10.3390/app6030078

[55] Chernikov A, van der Zande AM, Hill HM, Rigosi AF, Velauthapillai A, Hone J, Heinz TF. Electrical tuning of exciton binding energies in monolayer WS_2. Physical Review Letters. 2015;**115**:126802

[56] Geim AK, Grigorieva IV. Van der Waals heterostructures. Nature. 2013;**499**:419-425

[57] Rhyee J-S, Kwon J, Dak P, Kim J-H, Kim SM, Park J, Hong YK, Song W, Omkaram I, Alam MA. High mobility transistors based on large area and highly crystalline CVD grown $MoSe_2$ films on insulating substrates. Advanced Materials. 2016;**28**:2316-2321

[58] Sze SM, Ng KK. Physics of Semiconductor Devices. Hoboken, NJ: John Wiley & Sons, Inc.; 2006

[59] Koppens FHL, Mueller T, Avouris P, Ferrari AC, Vitiello MS, Polini M. Photodetectors based on graphene, other two-dimensional materials and hybrid systems. Nature Nanotechnology. 2014;**9**:2571-2574

[60] Lee EJH, Balasubramanian K, Weitz RT, Burghard M, Kern K. Contact and edge effects in graphene devices. Nature Nanotechnology. 2008;**3**:486-490

[61] Lou Z, Liang Z, Shen G. Photodetectors based on two dimensional materials. Journal of Semiconductors. 2016;**37**:9

[62] Freitag M, Low T, Xia F, Avouris P. Photoconductivity of biased graphene. Nature Photonics. 2013;**7**:53-59

[63] Saleh BEA, Teich MC, Saleh BE. Fundamentals of Photonics. New York: Wiley; 1991

[64] Rappaport P. The photovoltaic effect and its utilization. Solar Energy. 1959;**3**:8-18

[65] Furchi MM, Polyushkin DK, Pospischil A, Mueller T. Mechanisms of photoconductivity in atomically thin MoS_2. Nano Letters. 2014;**14**(11):6165-6170

[66] Buscema M, Barkelid M, Zwiller V, van der Zant HSJ, Steele GA, Castellanos-Gomez A. Large and tunable photothermoelectric effect in single-layer MoS_2. Nano Letters. 2013;**13**:358-363

[67] Wei P, Bao WZ, Pu Y, Lau CN, Shi J. Anomalous thermoelectric transport of Dirac particles in graphene. Physical Review Letters. 2009;**102**:166808

[68] Zuev YM, Chang W, Kim P. Thermoelectric and magnetothermoelectric transport measurements of graphene. Physical Review Letters. 2009;**102**:096807

[69] Li Z, Bae MH, Pop E. Substrate-supported thermometry platform for nanomaterials like graphene, nanotubes and nanowires. Applied Physics Letters. 2014;**105**(2):023107

[70] Wu J, Schmidt H, Amara KK, et al. Large thermoelectricity via variable range hopping in chemical vapour deposition grown single-layer MoS_2. Nano Letters. 2014;**14**(5):2730-2734

[71] Bhushan B. Springer Handbook of Nanotechnology. New York: Springer; 2007

[72] Nolas GS, Sharp J, Goldsmid J. Thermoelectrics: Basic Principles and New Materials Developments. New York: Springer; 2001

[73] Jyh MW, Wei EC. Ultrahigh responsivity and external quantum efficiency of an ultraviolet-light photodetector based on a single VO_2 microwire. ACS Applied Materials & Interfaces. 2014;**6**:14286-14292

[74] Choi MS, Qu D, Lee D, Liu X, Watanable K, Taniguchi T, Yoo WJ. Lateral MoS_2 p–n junction formed by chemical doping for use in high-performance optoelectronics. ACS Nano. 2014;**8**:9332-9340

[75] Mao J, Yu Y, Wang L, Zhang X, Wang Y, Shao Z, Jie J. Ultrafast, broadband photodetector based on $MoSe_2$/silicon heterojunction with vertically standing layered structure using graphene as transparent electrode. Advancement of Science. 2016;**3**:1600018

[76] Schroder DK. Semiconductor Material and Device Characterization. 3rd ed. New Jersey: John Wiley & Sons; 2006

[77] Jha AR. Infrared Technology. New York: Wiley; 2000. pp. 245-359

[78] Bhattacharya P. Semiconductor Optoelectronics Device. Upper Saddle River, NJ: Prentice-Hall; 1997. pp. 345-367

[79] Bube RH. Photoconductivity of Solids. New York: John Wiley; 1960. p. 1

[80] Jinhua L, Liyong N, Zijian Z, Feng Y. Photosensitive graphene transistors. Advanced Materials. 2014;**26**:5239-5273

[81] Perea-López N, Elías AL, Berkdemir A, Castro-Beltran A, Gutiérrez HR, Feng S, Lv R, Hayashi T, López-Urías F, Ghosh S, Muchharla B, Talapatra S, Tereones H, Terrones M. Photosensor device based on few-layered WS_2 films. Advanced Functional Materials. 2013; **23**(44):5511-5517

[82] Radisavljevic B, Radenovic A, Brivio J, Giacometti V, Kis A. Single-layer MoS_2 transistors. Nature Nanotechnology. 2011;**6**:147-150

[83] Riikonen J, Tuomi T, Lankinen A, Sormunen J, Saynatjoki A, Knuuttila L, Lipsanen H, McNally PJ, O'Reilly L, Danilewsky A, Sipila H, Vaijarvi S, Lumb D, Owens A. Synchrotron X-ray topography study of defects in indium antimonide P-I-N structures grown by

metal organic vapour phase epitaxy. Journal of Materials Science: Materials in Electronics. 2005;**116**:449-453

[84] Bolotin KI, Sikes KJ, Jiang Z, Klima M, Fudenberg G, Hone J, Kim P, Stormer HL. Ultrahigh electron mobility in suspended graphene. Solid State Communications. 2008; **146**:351-355

[85] Wang X, Gong Y, Shi G, Chow WL, Keyshar K, Ye G, Vajtai R, Lou J, Liu Z, Ringe E. Chemical vapor deposition growth of crystalline monolayer $MoSe_2$. ACS Nano. 2014; **8**:5125-5131

[86] Kumar N, Cui Q, Ceballous F, He D, Wang Y, Zhao H. Exciton diffusion in monolayer and bulk $MoSe_2$. Nanoscale. 2014;**6**:4915-4919

[87] Dean CR, Young AF, Meric I, Lee C, Wang L, Sorgenfrei S, Watanabe K, Taniguchi T, Kim P, Shepard K, et al. Boron nitride substrates for high-quality graphene electronics. Nature Nanotechnology. 2010;**5**:722-726

[88] Lee G-H, Yu Y-J, Cui X, Petrone N, Lee C-H, Choi MS, Lee D-Y, Lee C, Yoo WJ, Watanabe K, et al. Flexible and transparent MoS_2 field-effect transistors on hexagonal boron nitride-graphene heterostructures. ACS Nano. 2013;**7**:7931-7936

[89] Mekki A, Dere A, Mensah-Darkwa K, Al-Ghamdi A, Gupta RK, Harrabi K, Farooq WA, El-Tantawy F, Yakuphanoglu F. Graphene controlled organic photodetectors. Synthetic Metals. 2016;**217**:43-56

[90] Liu E, Long M, Zeng J, Luo W, Wang Y, Pan Y, Zhou W, Wang B, Hu W, Ni Z, You Y, Zhang X, Qin S, Shi Y, Watanable K, Taniguchi T, Yuan H, Hwang HY, Cui Y, Miao F, Xing D. High responsivity phototransistors based on few-layer ReS_2 for weak signal detection. Advanced Functional Materials. 2016;**26**:1938-1944

[91] Tosun M, Chuang S, Fang H, Sachid AB, Hettick M, Lin Y, Zeng Y, Javey A. High-gain inverters based on WSe_2 complementary field-effect transistors. ACS Nano. 2014;**8**:4948-4953

[92] Hwang WS, Remskar M, Yan R, Protasenko V, Tahy K, Chae SD, Zhao P, Konar A, Xing H, Seabaugh A, Jena D. Transistors with chemically synthesized layered semiconductor WS2 exhibiting 105 room temperature modulation and ambipolar behaviour. Applied Physics Letters. 2012;**101**:013107

[93] Larentis S, Fallahazad B, Tutuc E. Field-effect transistors and intrinsic mobility in ultra-thin $MoSe_2$ layers. Applied Physics Letters. 2012;**101**:223104

[94] Fathipour S, Ma N, Hwang WS, Protasenko V, Vishwanath S, Xing HG, Xu H, Jena D, Appenzeller J, Seabaugh A. Exfoliated multilayer $MoTe_2$ field-effect transistors. Applied Physics Letters. 2014;**105**:192101

[95] Ayari A, Cobas E, Ogundadegbe O, et al. Realization and electrical characterization of ultrathin crystals of layered transition-metal dichalcogenides. Journal of Applied Physics. 2007;**101**(1):14507

[96] Zhang W, Huang JK, Chen CH, et al. High-gain photo transistors based CVD MoS_2 monolayer. Advanced Materials. 2013;**25**(25):3456-3461

[97] Zhan Y, Liu Z, Najmaei S, Ajayan PM, Lou J. Large-area vapor-phase growth and characterization of MoS_2 atomic layers on a SiO_2 substrate. Small. 2012;**8**:966-971

[98] Liu KK, Zhang W, Lee YH, Lin YC, Chang MT, Su CY, Chang CS, Li H, Shi Y, Zhang H, Lai CS, Li LJ. Growth of large-area and highly crystalline MoS_2 thin layers on insulating substrates. Nano Letters. 2012;**12**:1538-1544

[99] Jung C, Kim SM, Moon H, Han J, Kwon J, Hong YK, Omkaram I, Yoon Y, Kim S, Park J. Highly crystalline CVD-grown multilayer $MoSe_2$ thin film transistor for fast photodetector. Scientific Reports. 2015;**5**:15313

[100] Chang Y-H, Zhang W, Zhu Y, Han Y, Pu J, Chang J-K, Hsu W-T, Huang J-K, Hsu C-L, Chiu M-H, Takenobu T, Li H, Wu C-I, Chang W-H, Wee ATS, Li L-J. Monolayer $MoSe_2$ grown by chemical vapor deposition for fast photodetection. ACS Nano. 2014;**8**:8582-8590

[101] Xia J, Huang X, Liu L-Z, Wang M, Wang L, Huang B, Zhu D-D, Li J-J, Gu C-Z, Meng X-M. CVD synthesis of large-area, highly crystalline $MoSe_2$ atomic layers on diverse substrates and application to photodetectors. Nanoscale. 2014;**6**:8949-8955

[102] Duan X, Wang C, Shaw JC, Cheng R, Chen Y, Li H, Wu X, Tang Y, Zhang Q, Pan A. Lateral epitaxial growth of two-dimensional layered semiconductor heterojunctions. Nature Nanotechnology. 2014;**9**:1024-1030

[103] Huo N, Yang S, Wei Z, et al. Photoresponsive and gas sensing field-effect transistors based on multilayer WS_2 nanoflakes. Scientific Reports. 2014;**4**:5209

[104] Zhang W, Chiu MH, Chen CH, et al. Role of metal contacts in high-performance phototransistors based on WSe_2 monolayers. ACS Nano. 2014;**8**(8):8653-8661

[105] Hu P, Wen Z, Wang L, Tan P, Xiao K. Synthesis of few-layer GaSe nanosheets for high performance photodetectors. ACS Nano. 2012;**6**:5988-5994

[106] Yin L, Zhan X, Xu K, Wang F, Wang Z, Huang Y, Wang Q, Jiang C, He J. Ultrahigh sensitive $MoTe_2$ phototransistors driven by carrier tunnelling. Applied Physics Letters. 2016;**108**:043503

[107] Xu K, Wang Z, Wang F, Huang Y, Wang F, Yin L, Jiang C, He J. Ultrasensitive phototransistors based on few-layered HfS_2. Advanced Materials. 2015;**27**:7881-7887

[108] Yang S, Tongay S, Li Y, Yue Q, Xia J-B, Li S-S, Li J, Wei S-H. Layer-dependent electrical and optoelectronic responses of $ReSe_2$ nanosheet transistors. Nanoscale. 2014;**6**:7226-7231

[109] Zhang E, Jin Y, Yuan X, Wang W, Zhang C, Tang L, Liu S, Zhou P, Hu W, Xiu F. ReS_2-based field-effect transistors and photodetectors. Advanced Functional Materials. 2015;**25**:4076-4082

[110] Liu F, Zheng S, He X, Chaturvedi A, He J, Chow WL, Mion TR, Wang X, Zhou J, Fu Q, Fan HJ, Tay BK, Song L, He R-H, Kloc C, Ajayan PM, Liu Z. Highly sensitive detection of polarized light using anisotropic 2D ReS_2. Advanced Functional Materials. 2016;**26**: 1169-1177

[111] Hafeez M, Gan L, Li H, Ma Y, Zhai T. Large-area bilayer ReS_2 film/multilayer ReS_2 flakes synthesized by chemical vapor deposition for high performance photodetectors. Advanced Functional Materials. 2016;**26**:4551-4560

[112] Liu E, Long M, Zeng J, Luo W, Wang Y, Pan Y, Zhou W, Wang B, Hu W, Ni Z, You Y, Zhang X, Qin S, Shi Y, Watanabe K, Taniguchi T, Yuan H, Hwang HY, Cui Y, Miao F, Xing D. High responsivity phototransistors based on few-layer ReS_2 for weak signal detection. Advanced Functional Materials. 2016;**26**:1938-1944

[113] Shim J, Oh A, Kang DH, Oh S, Jang SK, Jeon J, Jeon MH, Kim M, Choi C, Lee J, Lee S, Yeom GY, Song YJ, Park J-H. High-performance 2D rhenium disulfide (ReS_2) transistors and photodetectors by oxygen plasma treatment. Advanced Materials. 2016;**28**:6985-6992

[114] Hu P, Zhang J, Yoon M, Qiao X-F, Zhang X, Feng W, Tan P, Zheng W, Liu J, Wang X, Idrobo JC, Geohegan DB, Xiao K. Highly sensitive phototransistors based on two-dimensional GaTe nanosheets with direct band gap. Nano Research. 2014;**7**:694-703

[115] Liu F, Shimotani H, Shang H, Kanagasekaran T, Zólyomi V, Drummond N, Fal'ko VI, Tanigaki K. High-sensitivity photodetectors based on multilayer GaTe flakes. ACS Nano. 2014;**8**:752-760

[116] Hu PA, Wang LF, Yoon M, Zhang J, Feng W, Wang XN, Wen ZZ, Idrobo JC, Miyamoto Y, Geohegan DB, Xiao K. Highly responsive ultrathin GaS nanosheet photodetectors on rigid and flexible substrates. Nano Letters. 2013;**13**:1649-1654

[117] Tao Y, Wu X, Wang, et al. Flexible photodetector from ultraviolet to infrared based on SnS_2 nonosheet microsphere film. Journal of Materials Chemistry C. 2015;**3**(6):1347-1353

[118] Tao Y-R, Wu X-C, Xiong W-W. Flexible visible-light photodetectors with broad photoresponse based on ZrS_3 nanobelt films. Small. 2014;**10**:4905-4911

[119] Tao Y-R, Wu J-J, Wu X-C. Enhanced ultraviolet-visible light responses of phototransistors based on single and a few ZrS_3 nanobelts. Nanoscale. 2015;**7**:14292-14298

[120] Xiong W-W, Chen J-Q, Wu X-C, Zhu J-J. Individual HfS_3 nanobelt for field-effect transistor and high performance visible-light detector. Journal of Materials Chemistry C. 2014;**2**:7392-7395

[121] Xiong W-W, Chen J-Q, Wu X-C, Zhu J-J. Visible light detectors based on individual $ZrSe_3$ and $HfSe_3$ nanobelts. Journal of Materials Chemistry C. 2015;**3**:1929-1934

[122] Xie LM. Two-dimensional transition metal dichalcogenide alloys: Preparation, characterization and applications. Nanoscale. 2015;**7**:18392-18401